Evaluation of Wind Effect on Adjacent Tall Buildings

Vikramsingh Bhosale[1], M. R. Shiyekar[2]
[1]G Student, Applied Mechanics Department, Government College of Engineering, Karad, Maharashtra, India.
[2]Adjunct Professor, Applied Mechanics Department, Government College of Engineering, Karad, Maharashtra, India

Abstract—**The study of wind effects on adjacent tall buildings is essential for ensuring building safety, performance, and resilience in urban environments, particularly in light of increasing severe weather events associated with climate change. This paper evaluates the application of Fluid-Structure Interaction (FSI) techniques in simulating wind behavior and structural responses of high-rise buildings. FSI analysis assesses the dynamic responses of buildings under wind-induced forces and deformations. The method offers a more accurate and comprehensive framework for evaluating the wind-structure interactions, particularly when multiple tall buildings are in close proximity. However, the implementation of FSI methods presents challenges, including high computational costs and the sensitivity of results to input parameters, which require rigorous validation through experimental data. The findings provide valuable insights into fluid-structure interaction (FSI) effects, offering opportunities to enhance the safety and performance of high-rise buildings. The results also emphasize the need for ongoing research to further optimize building design under dynamic wind conditions, ensuring safer, more resilient structures in rapidly evolving urban landscapes.**

Index Terms—**Wind Engineering, Tall Buildings, Fluid-Structure Interaction (FSI), Structural Response**

I. INTRODUCTION

The evaluation of wind effects on adjacent tall buildings using Fluid-Structure Interaction (FSI) is a critical area of study within wind engineering, emphasizing how wind influences the performance and safety of high-rise structures. As urban environments become denser and more vertically oriented, understanding the complex interactions between wind and buildings is increasingly important. The integration of FSI methods enables engineers to simulate wind behavior and assess structural responses with greater accuracy than traditional techniques, providing valuable insights for designing robust urban infrastructure. When combined with aerodynamic analysis, FSI offers a comprehensive framework for evaluating how wind-induced forces impact structural integrity, especially when multiple tall buildings are located in close proximity. This approach helps engineers anticipate and mitigate potential issues such as vibrations, oscillations, and dynamic deformations caused by wind interactions. However, the application of FSI remains technically demanding, requiring advanced computational resources and interdisciplinary expertise.

While these computational techniques offer significant advantages, they also involve high computational costs and sensitivity to input parameters, necessitating rigorous validation against experimental data to ensure accuracy and reliability in predictions. Furthermore, there are ongoing debates regarding the need to refine existing design codes to incorporate insights derived from simulations, highlighting the necessity for a paradigm shift in how wind loads are assessed and integrated into building design practices. As architectural trends favor taller and more slender buildings, the implications of wind-structure interactions become increasingly pertinent. Research has shown that effective modeling of these interactions can lead to enhanced safety and performance in high-velocity wind conditions, ultimately benefiting the occupants and surrounding communities. The evolving nature of FSI methodologies signifies a pivotal advancement in wind engineering, paving the way for more robust and resilient structures in urban landscapes.

Wind interference occurs when the disturbed flow field around one structure affects the loads and responses of another nearby structure, often quantified through an interference factor (IF) or aerodynamic

interference factor (AIF). Fluid–structure interaction analyses are broadly classified as:

One-way FSI: the CFD solver feeds pressure loads to the structural solver but ignores structural feedback to the flow.

Two-way FSI: pressures and structural deformations are exchanged bidirectionally at every time step, capturing aeroelastic effects such as vortex-induced vibration (VIV) and galloping.

1.1 Overview of Wind Engineering

Wind engineering is a specialized discipline focused on understanding the interaction between wind and structures, including tall buildings and bridges. The significance of this field lies in its role in ensuring the safety, durability, and resilience of structures against wind-related hazards, which have become increasingly critical as urban environments evolve and climate change leads to more severe weather events.

Wind engineering encompasses the study of how wind affects the built environment and the design of structures to withstand wind loads. It involves integrating principles from aerodynamics, structural dynamics, and meteorology to predict wind pressures, velocities, and turbulence around buildings. A vital aspect of wind engineering is the accurate analysis of wind loads, which can vary significantly based on building height, shape, and neighboring structures.

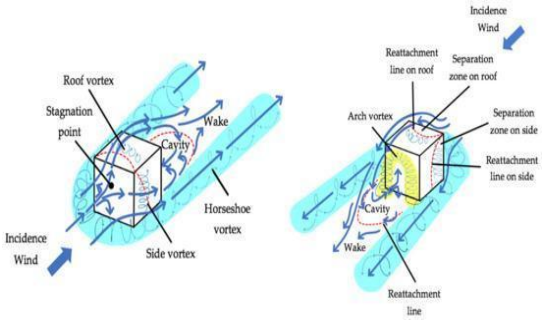

Figure 1. Wind Flow around Building

Understanding the wind-induced responses of adjacent tall buildings is crucial, as the presence of one structure can alter the wind flow patterns experienced by another. Factors such as building orientation, height, and spacing can affect the wind pressure distribution and the overall performance of structures. Consequently, studies utilizing Fluid-Structure Interaction (FSI) analysis are imperative for developing design strategies that mitigate potential wind-induced vibrations and ensure the structural integrity.

II. METHODOLOGY

To study structural responses, force and stresses at the building base were extracted over a simulation time of 20 seconds. Additionally, pressure contours and displacement values were analyzed to understand localized aerodynamic effects and wind-induced oscillations.

Two configurations were analyzed:

Single Isolated Building: To study the full exposure of wind impact without interference from nearby structures.

Grouped Tall Buildings: To assess shielding, channeling, and interference effects due to neighboring buildings.

The comparative evaluation between the two scenarios enabled us to identify critical insights regarding wind shielding, amplification effects in canyon-like formations, and the resulting structural stress variations. These findings are vital for optimizing building layouts in dense urban environments to minimize wind loads and ensure structural safety.

2.1 Atmospheric Boundary Layer and Interference Mechanisms

1. Computational Framework and Overview

This study was conducted using ANSYS Workbench 2021 R2, integrating ANSYS Fluent for fluid simulations and ANSYS Transient Structural for Force Reaction, deformation & Stress Distribution analysis under wind loading. The objective is to analyze and compare wind-induced aerodynamic and structural responses of a high-rise building in two configurations: a single isolated structure and a grouped arrangement in proximity to neighboring buildings.

The simulations consider two-way Fluid–Structure Interaction (FSI), enabling a coupled analysis of aerodynamic loading and structural deformation. FSI was executed using the System Coupling module within ANSYS Workbench.

2. Governing Fluid-Flow Equations (ANSYS Fluent Module)

The CFD simulations solve the Reynolds-Averaged Navier–Stokes (RANS) equations for incompressible, steady-state, turbulent airflow, assuming constant air properties at 20 °C.

Continuity Equation

$$\nabla \cdot \vec{u} = 0$$

Where:

$\vec{u}$ = velocity vector (m/s)

Momentum Equation (Navier–Stokes for incompressible flow)

$$\rho\left(\frac{\partial \vec{u}}{\partial t}+\vec{u}\cdot\nabla\vec{u}\right)=-\nabla p+\mu\nabla^2\vec{u}+\vec{f}$$

Where:

$\rho = 1.225\,\mathrm{kg/m^3}$ (air density)

$\mu = 1.79\times10^{-5}\,\mathrm{Pa}$ (dynamic viscosity of air)

p = static pressure (Pa)

$\vec{f}$ = body force vector (gravity often neglected for external flow)

Turbulence Model: Standard **k–ε**

The closure of RANS equations was achieved using the Standard k–ε turbulence model, governed by two additional transport equations:

Turbulent kinetic energy (k):

$$\frac{\partial k}{\partial t}+u_j\frac{\partial k}{\partial x_j}=\frac{\partial}{\partial x_j}\left[\left(\mu+\frac{\mu_t}{\sigma_k}\right)\frac{\partial k}{\partial x_j}\right]+G_k-\varepsilon$$

Turbulent dissipation rate (ε):

$$\frac{\partial \varepsilon}{\partial t}+u_j\frac{\partial \varepsilon}{\partial x_j}=\frac{\partial}{\partial x_j}\left[\left(\mu+\frac{\mu_t}{\sigma_\varepsilon}\right)\frac{\partial \varepsilon}{\partial x_j}\right]+C_{1\varepsilon}\frac{\varepsilon}{k}G_k-C_{2\varepsilon}\frac{\varepsilon^2}{k}$$

Standard Constants:

$C_\mu = 0.09$

$C_{1\varepsilon} = 1.44$

$C_{2\varepsilon} = 1.92$

$\sigma_k = 1.0\,\sigma_\varepsilon = 1.3$

3. Pressure Coefficient Calculation

To quantify the aerodynamic loading on the building surfaces, the pressure coefficient (Cp) was evaluated as:

$$C_p=\frac{P-P_{\mathrm{ref}}}{\frac{1}{2}\rho U^2}$$

Where:

P = local static pressure (Pa)

P_{ref} = reference pressure at inlet (Pa)

$\rho = 1.225\,\mathrm{kg/m^3}$

U = free-stream wind velocity (m/s)

4. Structural Modeling for FSI

The building's primary structure was modeled using a linear-elastic isotropic formulation, assuming rigid walls in CFD and flexible behavior in the structural solver. Base reactions obtained from Fluent were coupled to Static Structural through System Coupling, enabling two-way FSI.

Material Properties:

Property	Value
Density (ρ_s)	2390 kg/m³ (concrete)
Young's Modulus (E)	30 GPa
Poisson's Ratio (ν)	0.2

Wall Motion Equation (for dynamic mesh interface):

$$\rho_s\frac{\partial^2\vec{u}_s}{\partial t^2}=\nabla\cdot\sigma_s+\vec{f}_s$$

Where σ_s is the stress tensor and $\vec{f}_s$ is body force vector for the solid domain.

5. Fluid–Structure Interface Conditions

At the interface between fluid and solid domains:

- No-slip and no-penetration conditions were imposed.
- Displacement continuity was enforced using dynamic mesh techniques in Fluent and mesh morphing algorithms.

6. Mesh Generation and Convergence Criteria

A structured hexahedral mesh was generated using ANSYS Meshing with local refinement zones near the walls and wake regions to capture steep gradients.

Mesh Refinement Zones:

1. 10 layers of inflation mesh on wall boundaries
2. Mesh element count ranged from 1.2 to 2.8 million across configurations

7. Simulation Configuration and Boundary Conditions

Configurations Analyzed:

1. Single Isolated Building
2. Grouped Buildings

Boundary Conditions:

Boundary	Type	Value
Inlet	Velocity Inlet	50 m/s (uniform)
Outlet	Pressure Outlet	0 Pa (gauge)
Ground & Walls	No-slip Wall	Roughness height = 0.03 m
Top & Sides	Symmetry	

8. Output Parameters and Simulation Time

The CFD simulation was run for 20 seconds using transient solver settings, with a time step of 0.01 s.

The following parameters were extracted:

1. Velocity and pressure contours
2. Base shear
3. Deformation and stress distribution (via FSI)

Geometry of the Building(s) and Computational Domain

Single Isolated building = Building A

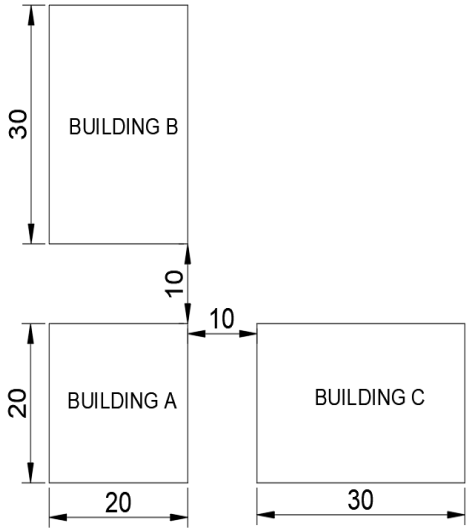

Figure 2. Geometry of the Grouped Tall Buildings in the Computational Domain

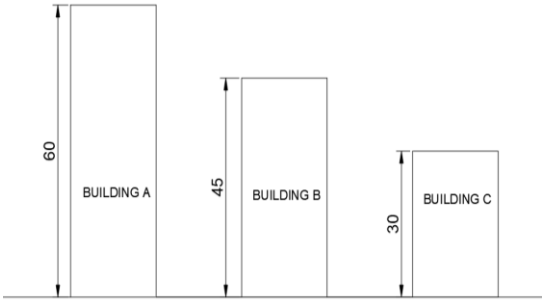

Figure 3. Geometry of the Grouped Tall Buildings in the Computational Domain

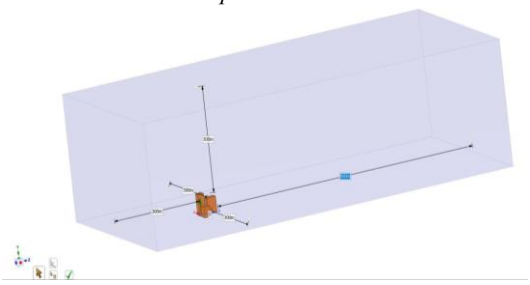

Figure 4. Domain Size of the Grouped Configuration

1. Upstream length: 5H
2. Downstream length: 15H
3. Lateral clearance: 5H on each side
4. Vertical clearance: 5H above the building top Height of highest building: 60m

Wind Profile

1. Uniform inlet velocity: A constant value of 50 m/s at the inlet

A uniform wind speed of 50 m/s was applied at the inlet, based on IS 875: Part III (2015) for Terrain Category 1 and a structure height of 60 m. Due to negligible wind variation over height at this scale, a UDF was not used, and a constant velocity profile was assumed.

2. Basic Wind speed: Vb= 50 m/s.
3. Code Provisions: IS 875: Part III 2015

$$V_z = V_b \times k_1 \times k_2 \times k_3 \times k_4$$

$$V_z = 50 \times 1.0 \times 1.0 \times 1.0 \times 1.0 = \boxed{50\,\mathrm{m/s}}$$

III. RESULTS AND DISCUSSION

A. Wind Analysis – Single Isolated Building

1. Pressure Distribution

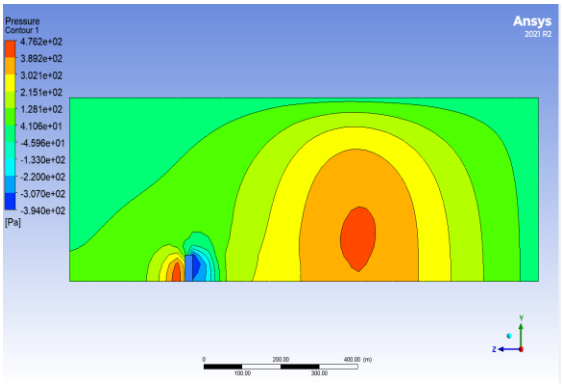

Figure 5. Pressure Distribution on Windward and Leeward Faces (Isolated Case)

1. Peak pressure increased from ~215 Pa to ~476 Pa over 20s.
2. Minimum suction pressure (leeward) rose from –394 Pa to –104 Pa.
3. Trend shows symmetrical and near-linear pressure growth, indicating stable vortex-induced loading.

2. Velocity

1. Maximum wind velocity reached 50.35 m/s.

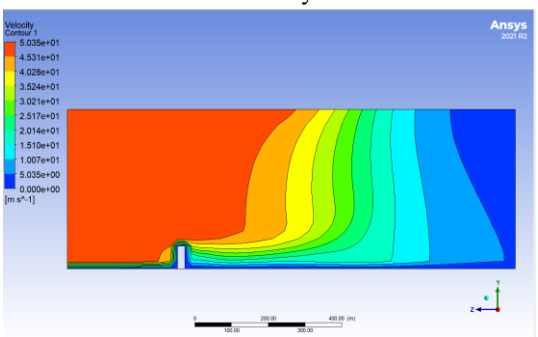

Figure 6. Velocity Contour Around an Isolated Tall Building

3. Total Force Reaction

1. Increased from ~4.71 × 10^5 N to ~1.54 × 10^6 N over 20s.
2. Indicates strong aerodynamic demand due to lack of shielding.

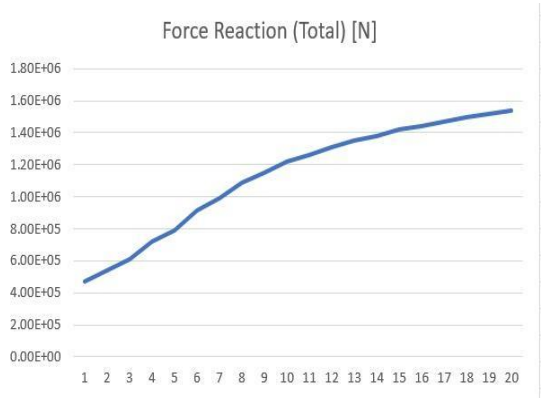

Figure 7. Force Reaction vs Time for Isolated Building

4. Structural Displacement

1. Max displacement rose from 0.044 mm to 0.1825 mm.

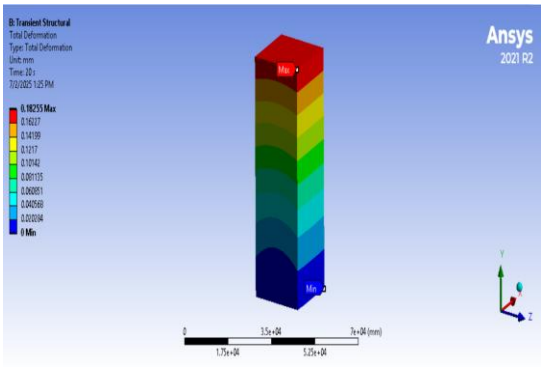

Figure 8. Total Deformation of Isolated Building under Wind Load

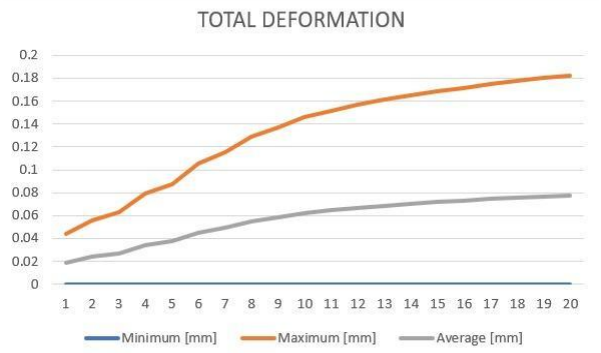

Figure 9. Total Deformation vs Time for Isolated Building

5. Stress Distribution

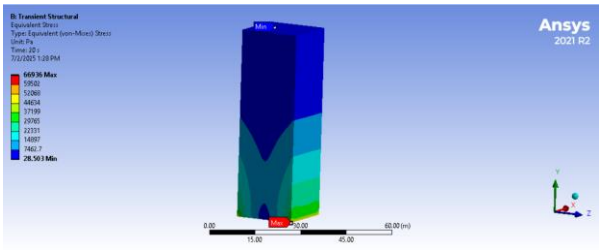

Figure 10. Equivalent Stress of Isolated Building under Wind Load

Figure 11. Equivalent Stress vs Time for Isolated Building

1. Max von Mises stress: ~66.9 kPa; average: ~7.6 kPa at 20s.
2. Stress gradually increased due to wind-induced bending and shear.

B. Wind Analysis – Grouped Buildings

1. Pressure Distribution

1. Max pressure: 1552 Pa (upwind faces); Max suction: –58.22 Pa.
2. Average pressure dropped to ~1250–1350 Pa, showing stabilization.
3. Suction remained dominant near leeward and side faces.

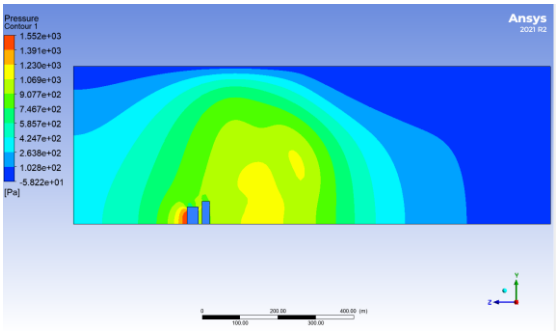

Figure 12. *Pressure Distribution on Windward and Leeward Faces – Grouped Configuration*

2. Velocity

1. Max velocity: 53.84 m/s.
2. Wake formation observed behind buildings.

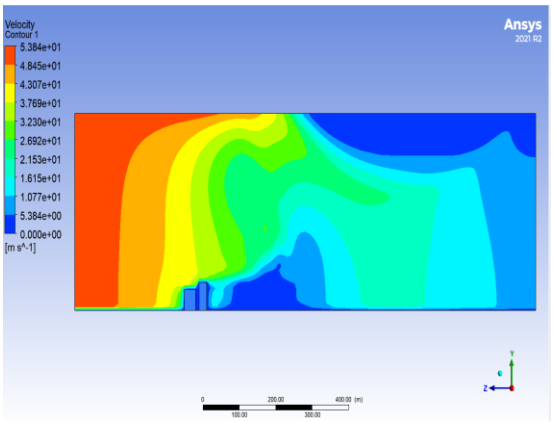

Figure 13. Velocity Contour Around Grouped Tall Buildings

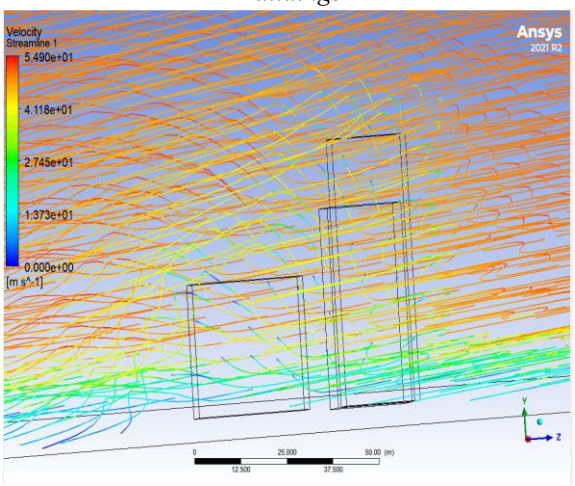

Figure 14. Velocity Streamlines Around Grouped Tall Buildings

3. Total Force Reaction

1. Started at ~1.17 × 10^7 N, dropped to ~1.61 × 10^6 N by 20s.
2. Decline suggests wake formation and aerodynamic shielding reduced loading.

Total Force Reaction vs Time:

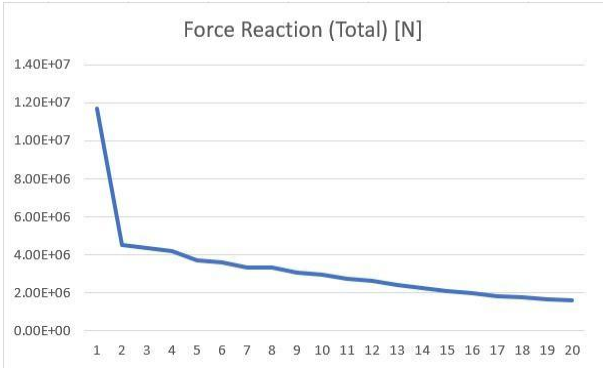

Figure 15. Force Reaction vs Time (0–20s) for Grouped Buildings

4. Deformations

1. Initial peak: 1.57 × 10^{-4} m, reducing to ~2.2–2.5 × 10^{-5} m. Indicates damped swaying as flow stabilizes.

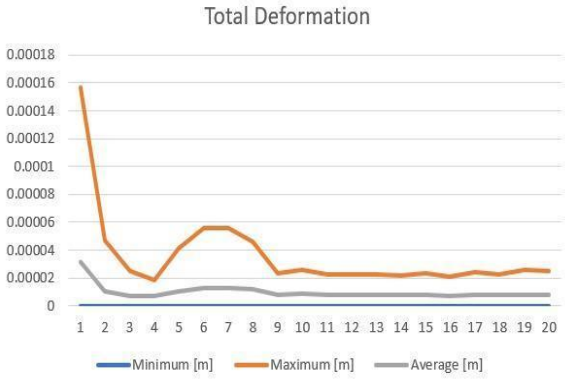

Figure 16. Total Deformation vs Time (0–20s) for Grouped Buildings

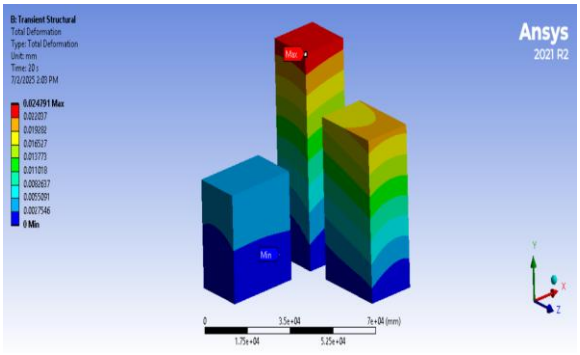

Figure 17. Total Deformation in Grouped Buildings

5. Stress Distribution

1. Max von Mises stress initially peaked at ~100 kPa, reducing to ~23 kPa by 20s.
2. Stress was highest during the first 2–3 seconds, then decreased exponentially.
3. The reduction became more gradual over time, indicating diminishing dynamic loads and stabilized internal stress response.

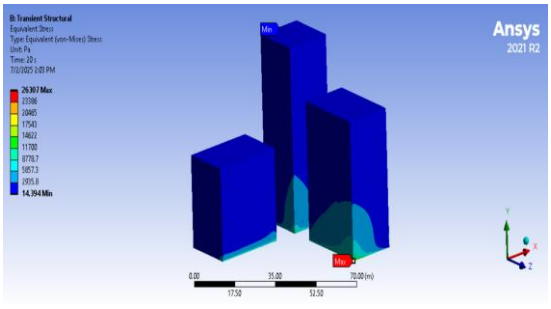

Figure 18. Equivalent Stress Distribution in Grouped Buildings

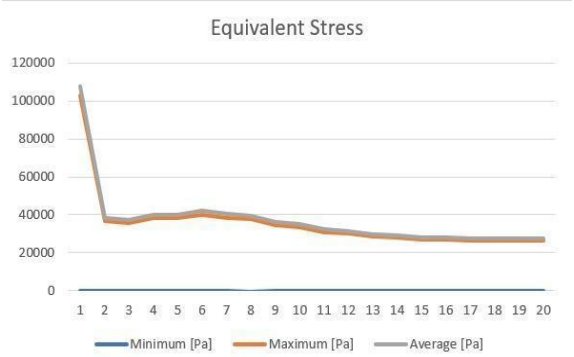

Figure 19. Equivalent Stress vs Time (0–20s) for Grouped Buildings

Comparative Assessment: Grouped vs. Single Isolated Building

The wind-induced effects on tall buildings vary significantly depending on their surrounding built environment. To quantify this influence, simulation results for both Grouped Buildings and a Single Isolated

Table 1. Comparative Results

Parameter	Isolated Building	Grouped Buildings
Max Pressure	476 Pa	1552 Pa (on upwind faces)
Max Suction	–394 Pa	–58.22 Pa
Max Velocity	50.35 m/s	53.84 m/s
Peak Reaction Force	1.54×10^6 N	1.17×10^7 N (initial), decreases to 1.61×10^6 N
Max Deformation	0.1825 mm	1.57×10^{-4} m (0.157 mm) initially, stabilizes to ~0.025 mm
Max von Mises Stress	100 kPa (initial), reduces to ~66.9 kPa at 20s	100 kPa (initial), reduces to ~26.3 kPa at 20s
Total Wind Load	Concentrated entirely on one structure	Distributed among multiple buildings
Flow Behavior	Direct exposure, vortex shedding	Wake formation, aerodynamic shielding

1. Pressure and Velocity: Grouped buildings encounter significantly higher wind pressure (1552 Pa vs. 476 Pa) and slightly greater peak velocities due to channeling and inter-building interference. However, they benefit from aerodynamic shielding in later stages.
2. Force Reactions: The isolated structure shows a steady increase in wind-induced base reaction force, reaching 1.54×10^6 N, whereas the grouped configuration starts with a much higher peak (1.17×10^7 N) that reduces sharply to 1.61×10^6 N, reflecting effective turbulence dissipation.
3. Displacement Behavior: The maximum deformation in the isolated case is 0.1825 mm, which is significantly larger than that in the grouped case (initially 0.157 mm, stabilizing to ~0.025 mm). This illustrates how shielding effects in grouped setups reduce building sway over time.
4. Stress Response: Both configurations initially show von Mises stress of around 100 kPa, but over time, the isolated building retains a higher residual stress (~66.9 kPa), while the grouped buildings drop to ~26.3 kPa. This suggests more efficient stress redistribution and damping in the grouped setup.
5. Flow Characteristics: The isolated building faces direct wind impact with regular vortex shedding, leading to sustained loading. In contrast, grouped buildings experience wake formation and shielding, which initially amplify forces but later stabilize the flow and reduce dynamic effects.

IV. CONCLUSION

Pressure and force responses in the grouped setup peak early but diminish rapidly, whereas they continue rising in the isolated case.

Structural deformation and von Mises stress are significantly higher and more sustained in the isolated building.

Flow behavior around grouped buildings shifts from turbulent interference to aerodynamic balance, highlighting the importance of spatial arrangement in wind-sensitive design.

Overall, the grouped configuration offers better aerodynamic performance and structural resilience under sustained wind loads. These insights are valuable for optimizing urban planning, tall building placement, and structural design in wind-prone regions.

V. LIMITATIONS

Rigid-Body Assumption:

The structure was modeled as rigid, and while some FSI coupling was included, dynamic responses like occupant perceived accelerations were not fully captured. A complete two-way FSI approach is needed for higher accuracy.

Single Wind Direction:

Only a 0° wind approach was considered. Realistic scenarios involve varying wind directions, which may significantly affect shielding and interference patterns.

Simplified Geometry:

Architectural features such as balconies, setbacks, and podiums were excluded. These can influence wind flow and pressure distribution in practical cases.

Lack of FSI Guidelines:

There is no standardized procedure for wind-structure FSI analysis. Future work should focus on developing validated guidelines and benchmark cases.

REFERENCES

[1] Gan, W., et al. (2024). Wind-Driven Dynamics Around Building Clusters: Impact of Convex and Concave Curvilinear Morphologies and Central Angles. Atmosphere.

[2] Qureshi, M., Zahid, I., & Iqbal, M. (2016). Pedestrian level wind environment assessment around a group of high-rise cross-shaped buildings: Effect of building shape, separation, and orientation. Building and Environment, 115, 115-124.

[3] Yadav, H., & Yadav, H. (2024). Wind-Induced Aerodynamic Responses of Triangular High-Rise Buildings with Varying Cross-Section Areas. Buildings.

[4] Priambodo, D., et al. (2020). Experimental Studies of Wind Flow Inside a Street Canyon Between High-Rise Buildings with Angle of Attack Modifications.

[5] Kim, Y., et al. (n.d.). The effects of geometrical changes of tall buildings on pedestrian-level wind speeds. Proceedings of the Eleventh International Conference on Engineering Computational Technology.

[6] Glumac, A., et al. (2018). University of Birmingham Wind energy potential above a high-rise building influenced by neighboring buildings: An experimental investigation.

[7] Lu, J., et al. (2023). Representing the effects of building height variability on urban canopy flow. Quarterly Journal of the Royal Meteorological Society.

[8] Vranešević, K. K., et al. (2023). LES study on the urban wind energy resources above the roof of buildings in generic cluster arrangements: Impact of building position. Journal of Wind Engineering and Industrial Aerodynamics.

[9] Toja-Silva, F., et al. (2015). On Roof Geometry for Urban Wind Energy Exploitation in High-Rise Buildings. De Computis.

[10] Yang, J., et al. (2020). Air pollution dispersal in high density urban areas: Research on the triadic relation of wind, air pollution, and urban form.

[11] Mao, Z., et al. (2020). Aerodynamic Performance Analysis of a Building-Integrated Savonius Turbine. Energies.

[12] Lu, W., et al. (2023). Effects of side and corner modification on the aerodynamic behavior of high-rise buildings considering serviceability and survivability. Journal of Wind Engineering and Industrial Aerodynamics.

[13] Amin, J. (2010). Aerodynamic Modifications to the Shape of the Buildings: A Review of the State-of-the-Art.

[14] Juan, Y., et al. (2024). Improvement of wind energy potential through building corner modifications in compact urban areas. Journal of Wind Engineering and Industrial Aerodynamics.

[15] Kasana, D., et al. (2022). Evaluation of aerodynamic effects on a tall building with various cross-section shapes having equal area. Forces in Mechanics.

[16] Bharat, A. (2012). Effects of High-Rise Building Complex on the Wind Flow Patterns on Surrounding Urban Pockets.
[17] Priambodo, D., et al. (2020). Experimental Studies of Wind Flow Inside a Street Canyon Between High-Rise Buildings with Angle of Attack Modifications. DOI: [Link]
[18] Lu, W., et al. (2023). Effects of side and corner modification on the aerodynamic behavior of high-rise buildings considering serviceability and survivability. Journal of Wind Engineering and Industrial Aerodynamics.
[19] Yadav, H., et al. (2024). Wind-Induced Aerodynamic Responses of Triangular High-Rise Buildings with Varying Cross-Section Areas. Buildings.
[20] an, B., et al. (2022). Numerical Simulation for Vortex-Induced Vibration (VIV) of a High-Rise Building Based on Two-Way Coupled Fluid-Structure Interaction Method. International Journal of Structural Stability and Dynamics.
[21] Wijesooriya, K., et al. (2020). An uncoupled fluid-structure interaction method in the assessment of structural responses of tall buildings.
[22] Liu, Z., et al. (2023). Along-wind and across-wind coupling analysis of high-rise buildings: Modeling and parameter identifications. Journal of Building Engineering.
[23] Tu, J., et al. (2015). Computational Fluid Structure Interaction.
[24] Revuz, J. (2011). Numerical simulation of the wind flow around a tall building and its dynamic response to wind excitation.
[25] Sabharwal, R., et al. (2023). Structural Stability Analysis of Multistory Building Structure under Wind Load Conditions. International Journal of Innovative Research in Engineering & Management.
[26] Wijesooriya, K., et al. (2020). Wind loads on a super-tall slender structure: A validation of an uncoupled fluid-structure interaction (FSI) analysis.
[27] Revuz, J., et al. (2009). Numerical Simulation of the Dynamic Wind Loading on and Response of Tall Buildings.
[28] Vîlceanu, V., et al. (2023). Coupled numerical simulation of liquid sloshing dampers and wind–structure simulation model. Journal of Wind Engineering and Industrial Aerodynamics.
[29] Jagadale, Anand Lalasaheb and Mitkari, Pankaj and Chougule, Vikas and Roy, Pavel and Lulla, Vinit, Understanding Effects of Blood Viscosity on Artery Wall Using FSI and CFD Simulations (2024)